AN EXPERIMENTAL INVESTIGATION OF LEADING-EDGE SPANWISE BLOWING

Su Wenhan,† Liu Mouji,* Zhou Bocheng,† Qiu Chenghao,† Xiong Shanwen†
Beijing Institute of Aeronautics and Astronautics
Beijing, China

Abstract

Oil flow Visualizations and pressure measurements on a 30° swept trapezoidal wing were conducted to investigate the leading-edge spanwise blowing (LE SWB), which is very near the leading edge and along it. The LE SWB can provide higher maximum lift coefficient than conventional SWB. It can generate a more stable jet leading-edge vortex above the inboard wing, and the outboard wing leading-edge vortex can also be enhanced. The flow patterns of the wing with LE SWB are similar to those of a strake-wing.

Nomenclature

b/2	Wing semi-span(the word "wing" always means the "exposed wing" of the model in this paper)
c	Wing local chord
c_r	Wing root chord
c_l	Section lift coefficient
C_L	Lift coefficient of wing
C_p	Pressure coefficient
C_μ	Jet momentum coefficient
x	Chordwise distance, measured from wing leading edge
x_n	Chordwise distance of nozzle from leading edge of wing root chord
x_n/c_r	Dimensionless chordwise distance of nozzle
z	Spanwise distance, measured from wing-body-juncture
α	Angle of attack

Subscripts:

l	condition on lower surface of wing
u	condition on upper surface of wing

*Professor.
†Lecturer.

Introduction

For designing the current fighter aircraft, it is very important to increase its high-angle-of-attack aerodynamic characteristics. It has been found that spanwise blowing is a promising technique to achieve this objuctive. Spanwise blowing (SWB) as a means of controlling flow separation and leading-edge vortex has been investigated for many years [1-10]. In most of the previous investigations of spanwise blowing, the nozzle was located at points for which $x_n/c_r \geq 0.1$ and on the upper surface of the wing. Such a type of spanwise blowing is called the conventional SWB in this paper. Some results of spanwise blowing on the lower surface of a leading-edge extension wing were presented[10].

In this paper, nozzle is located very near the leading edge and blowing is along it. This is called the leading-edge SWB. Fig.1 shows the completely separated flow and the leading-edge vortex flow. By means of conventional SWB the former can be changed into the latter as shown in Fig.1. For this case the reattached line A_2 is near (fore or aft) the nozzle. For leading-edge SWB, given in Fig.2, the nozzle is located near the primary separation line S_1. The flow near the separation line is accelerated spanwise so that a stable leading-edge vortex could be developed.

Bearing this in mind a conceptual study was carried out in the aerodynamics laboratory of BIAA[12]. This study is designed to explore the flow mechanism of the leading-edge SWB and to compare it with conventional SWB. The primary results of this study and some results from water tunnel

tests for strake-wing are presented.

Experimental Investigation

Model and Apparatus

The wind tunnel model consisted of a wing-body-horizontal tail combination. A two-view drawing of the model is shown in Fig.3, and a photograph of the model mounted in the wind tunnel is shown in Fig.4. The trapezoidal wing had a 30° leading edge sweep angle. The aspect ratio was 3.2. The wing was a flat plat with sharpened leading and trailing edges. On the upper surface of the left wing 152 pressure orifices were arranged in chordwise rows at eight different span locations. The right wing was used to take oil flow visualization. The air supply system and nozzle locations were also shown in Fig.3. The nozzle was a straight circular tube with inner diameter of 4 mm. The five nozzle chordwise locations tested were as follows: x_n/c_r= 0_l, 0.015_l, 0.15_u; 0.12, 0.32. where subscripts l and u refer to whether the nozzle is on the lower surface or on the upper surface of the wing, respectively. The former three were used to conduct leading-edge SWB, and the latter two were used to conduct conventional SWB. All of the nozzle heights were 0.75d (d-inner diamiter of the nozzle), and all the nozzle orientations were approximatly parallel to the wing leading edge.

Wind Tunnel Tests

The tests of pressure measurement and oil flow visualization were conducted in the BIAA 1.02×0.76 meter low speed wind tunnel which has an elliptic test section. The Reynolds number based on the mean aerodynamic chord of the wing was about 2×10^5. under the conditions of x_n/c_r= 0.015_l, 0.015_u, 0.12, 0.32, the wing surface pressures were measured at angles of attack from 4° to 32° at 4° increments. The oil flow visualizations were conducted for all the five nozzle locations and at angles of attack up to 42°.

The jet momentum coefficient C_μ=0.28, which is defined as:

$$C_\mu = \dot{m}V_j / q_\infty S$$

where S is the area of the wing; q_∞ is free-stream dynamic pressure; $\dot{m}$ is the measured mass flow rate; and V_j is the jet velocity reached by isentropic expansion from the stagnation pressure at the nozzle exit to free-stream static pressure, given by

$$V_j=44.83\sqrt{T_{oj}\left[1-\left(p_\infty/p_{oj}\right)^{2/7}\right]}\ \text{m/sec}$$

where the T_{oj} is in Kelvin.

Results and Discussions

Lift Characteristics

The pressure data were integrated to obtain lift coefficients. The wing-lift curves are presented in Fig.5. It shows that the leading-edge SWB(x_n/c_r=0.015_u, 0.015_l) can improve the lift characteristics at high angles of attack,and can provide higher maximum lift coefficient than conventional SWB (x_n/c_r=0.32, 0.12), but at low and moderate angles of attack, the lift coefficients of the former are lower than those of the latter.

The variations of section lift coefficient along the span are shown in Fig.6. it can be seen that, at higher angles of attack, at inboard wing the section lift coefficients of leading-edge SWB are higher than those of the conventional SWB but at outboard wing the fonmers are lower than the latters.

The Flow Mechanism of Leading-Edge SWB

The Principal Flow Character of the 30° Swept Wing without Blowing

From the oil flow visualization, tuft-probe observation and pressure measurement

on the wing upper surface, it has been understood that in a range of moderate angles of attack (for example, $\alpha=10^{\circ}$-16°) there is a bursted leading-edge vortex above the wing upper surface. A typlcal flow pattern and the pressure iso-bar of this vortex are shown in Fig.7a and 8a. The bursting point of this vortex is above the fore area of the inboard wing and proceeds forword successively to the wing apex with increased angle of attack. In this range of angles of attack the slop of wing lift curve decreases rapidly (see. Fig.5). As the angle of attack is further increased the wing flow pattern will changes into spiral flow (Fig.7b), reversed flow and completely separated flow successively. These flow patterns correspond to the complete stall of the wing. The right photograph in Fig.7a is from the water tunnel test. The test model was a single flat-plate wing with 30° sweptback and chamfered leading edge. The dye was injected into the flow field from the wing leading edge and the dye tubes were embeded in the test model and were connected with dye supply lines behind the wing trailing edge. This photograph shows that the bursting vortex mentioned above could also be seen in the water tunnel test.

Leading-Edge SWB on Upper Surface

Fig.9 shows some surface flow patterns for $x_n/c_r=0.015_u$. Corresponding pressure distributions are given in Fig.10. It has been found that as the angle of attack is increased, four flow types occur successively on the upper surface of the wing. They can be discribed as follows:

(1) Coexistence of jet leading-edge vortex and attached flow. It occurs at $0^{\circ}\leq\alpha<10^{\circ}$ (Figs.9a, 10a). there is a jet leading-edge vortex above the inner pannel of the wing, and on the outer panel the flow is attached or reattached behind a leading-edge bubble. The jet leading-edge vortex is caused by the spanwise jet being at the leading edge. The portion of the jet closed to the exit nozzle is with high momentum and has not been decayed yet. This portion of the jet has two effects on the free stream (the crossflow). It, on the one hand, has a "obstacle" effect, and so the flow would separate from it, and there would be some vorticities shedding from the "separation line", On the other hand, as usual, the jet has an entrainment effect. Due to this effect the flow over the jet is accelerated along the leading edge (or spanwise). Therefore, the conditions for forming a stable three-dimensional vortex could be provided. This is just the way in which the jet LE vortex has been formed, as shown in Fig.2. In Fig.9a, the two boundary lines of the jet path is evident. It bends downstream.

(2) coexistence of jet LE vortex and outer panel vortex. It occurs at $10^{\circ}\leq\alpha<18^{\circ}$. At $\alpha=10^{\circ}$(Fig.9b), an unstable bubble vortex begins to occur above the outer panel, which is formed from the leading edge separation of the outboard wing, and is called outer panel vortex. At $\alpha=14^{\circ}$ the bubble vortex is changed into a concentrated vortex. This is attributed to the favorable interaction from the jet LE vortex and the mixing effect of the jet. From Fig.9c it can be seen that the jet tends to move toward the leading edge and the outer portion of the jet is rolled into the outer panel vortex and mixing with it. In both Fig.10b and 10c two suction ridges indicate the two vortices, and there is a valley in between.

(3) The coalescence of jet LE vortex with outer panel vortex. It occurs at $18^{\circ}\leq\alpha\leq22^{\circ}$. The coalescence process present not only in the oil flow patterns (Figs.9d, 9e) but also in the figures of pressure iso-bar (Figs.10d, 10e). When the two vortices have coalesced only a single ridge is present. This process can also be detected by a tuft-probe. At $\alpha=22^{\circ}$ a strong concentrated vortex has been formed basically.

(4) Bursting vortex. It occurs at $22^{\circ} < \alpha < 42^{\circ}$. By using a tuft-probe it has been found that as α goes over about 22° the vortex bursting occurs at the trailing edge of the wing. For the condition of leading edge SWB, the bursting vortex has a significant character, that is the strength of fore portion of the bursting vortex has been increasing up to 32°. This can be understood from Figs.10e and 10f. This is primarily due to the special effect of a jet LE vortex.

Leading Edge SWB on Lower Surface

The flow patterns and pressure distributions are given in Fig.11). For $x_n/c_r = 0.015_l$, at low angles of attack ($\alpha < 10^{\circ}$) the jet and the jet LE vortex occur beneath the wing and bend downstream. The effect of this vortex on the lower surface flow pattern and pressure distribution can be seen from the figures for $\alpha = 4^{\circ}$. This is an unfavorable effect on the wing lift. As α goes over $10^{\circ}$the jet portion near the noz nozzle exit causes a jet leading-edge vortex above the inboard wing. At the same time, the outer portion of the jet bends upstream, and is rolled up in the outer panel vortex above the outboard wing. In this case, the jet would form a feeding sheet carrying vorticity and high momentum shedding from the leading edge and thus enhances the outer panel vortex. The two-vortex coalescence and vortex bursting are earlier, and the bursting point of the coalescing vortex moves to the apex of the wing more quickly, and so the corresponding lift coefficient decreases rapidly. this is undesirable. However, it seems that, this defect could be diminished or cancelled if the nozzle moves forward a little, just as Fig.11b shows.

For $x_n/c_r = 0_l$, (see Fig.11b) even if the angle of attack is lower, say $\alpha = 4^{\circ}$, the jet LE vortex occurs above the wing instead of that beneath it. And it is noted that at $\alpha = 36^{\circ}$ there is still a fair flow pattern on the inner panel of the wing. This suggests that the wing lift coefficient characteristics in the high angle range would be improved.

Comparison of LE SWB with Conventional SWB

Some oil flow patterns and pressure isobar for $x_n/c_r = 0.32$ (which represents conventional SWB) are given in Fig.12. And the positions of suction ridge and the pressure on it are given in Fig.13. and Fig.14. For the conventional SWB, the dominant effect on the flow field is due to the leading-edge vortex enhanced by SWB, and for the LE SWB, the two vortices and interactions between them play the dominant one. Fig.14 shows that at moderate angles of attack (about 12° to 20°) the suctions on the ridge for $x_n/c_r = 0.32$ rise more rapidly with increasing angle of attack than those for $x_n/c_r = 0.015_u$; but at high angles of attack (about 20° to 32°) the formers fall rapidly and the inner portion of the latter is still rising successively.

The Analogy of Flow Patterns of Wing with LE SWB to those of Wing with Strake

The surface flow patterns of the wing with strake have been presented in refernce 11. In recent years, in order to insight into the three-dimensional flow fields generated by a wing with strake. A water tunnel study was carried out[13] in BIAA, and some further wind tunnel tests were conducted as well. The typical flow patterns of the wing with strake from these tests are shown in Fig.15. The water tunnel model has the same leading-edge sweep angle as the wind tunnel model ($76^{\circ}/30^{\circ}$), but is a single wing without body. It has been understood that the flow mechanism of the strake-wing is related closely to the interaction of the strake vortex and the outer panel vortex. As the angle of attack

is increased, under the favorable interaction of strake vortex the type of the outer panel vortex would be changed from a bursting vortex into a concentrated vortex. With the further increasing angle of attack, the bursting points of the two vortices move upstream from the trailing edge to the apex and the kink of the wing respectively. Obviously, there are some analogies in the flow pattern as well as flow mechanism between the wing with LE SWB and the wing with strake. The jet LE vortex is just like the strake vortex, and the interactions between the jet LE vortex and the outer panel vortex are similar to those between the strake vortex and the outer panel vortex of the strake wing.

Conclusions

The results of present conceptual study lead to the following conclusions:

1. There are two types of spanwise blowing, the flow mechanisms of which are different. They may be called the conventional SWB and leading-edge SWB.

2. Under the conditions of the present tests, the leading-edge SWB provided higher maximum lift coefficient than conventional SWB.

3. The leading-edge SWB can generate a jet leading-edge vortex, which is stronger and more stable. This vortex and the spreading jet can enhance the outer panel vortex.

4. For leading-edge SWB, with increasing angle of attack four flow types occur successively on the upper surface of the wing, they are (1) Coexistence of jet LE vortex and attached flow, (2) Coexistence of jet LE vortex and outer panel vortex, (3) Coalescence of jet LE vortex with outer panel vortex, (4) Bursting vortex.

5. There are some analogies of the flow patterns of wing with LE SWB to thoes of wing with strake.

Acknowledgement

The authots wish to express appreciation to professor B. Laschka, F.R.G., Professor J.L. Stollery, U.K. and Mr. J.S. Gibson, U.S.A. for their helpfull discussions.

This paper is based on wind tunnel tests of spanwise blowing and water tunnel tests for strake wing. These investigations were down by the authors and their colleagues Li Zhifang, Lü Zhiyong, Deng Xueying, Hu Jizhong, Gao Xiankun, Shen Yuxi and Han Jiankui.

References

1. Dixon, C.J., "Lift Augmentation by Lateral Blowing Over a Lifting Surface," AIAA Paper No. 69-193, Feb.1969.
2. Cornish, J.J., III., "High lift Applications of Spanwise Blowing," ICAS Paper No.70-09 Seventh ICAS Congress, Rome, Sept. 1970.
3. Werle, H., and Gallon,M., "Flow Control by Cross Jet," NASA T T F-14, 584,1972.
4. Dixon, C.J., Theisen, J.G., and Scruggs, R.M., "Theoretical and Experimental Investigations of Vortex Lift Control by Spanwise Blowing, Volume I-Experimental Research," LG 73 ER-0169, Lockheed Aircraft Corp., Sept. 1973. (AD 771 296)
5. Bradley, R.G., and Wray, W.O., "A Conceptual Study of Leading-Edge vortex Enhancement by Blowing," J.Aircraft, Jan. 1974.
6. Campbell, J.F., "Effects of Spanwise Blowing on the Pressure Field and Vortex-Lift Characteristics of a 44° Swept Trapezoidal Wing, "NASA TN D-7907, June, 1975.
7. Campbell, J.F., "Augmentation of Vortex Lift by Spanwise Blowing," J. Aircraft, Sept. 1976.
8. Kneeth, S.L., Clarke, P., "Lift Augmentation on a moderately swept wing by Spanwise Blowing," The Aeronautical J.

Oct. 1976.

9. Staudacher, W., Laschka, B.; Poisson-Quinton, Ph., Ledy, J.P., "Effect of Spanwise Blowing in the Angle-of-Attack Regime $\alpha = 0 + 90^{\circ}$," ICAS Paper 78-A 1-02, 11th ICAS Congress, 1978.
10. Erickson, G.E., "Effect of Spanwise Blowing on the Aerodynamic Characteristics of a Half-Span 50°-Swept Cropped Delta wing Configuration," AIAA Paper No. 79-1859, 1979.
11. Liu Mouji et al., "Flow Patterns and Aerodynamic Characteristics of Wing With Strake," AIAA Paper No. 79-1877, Aug. 1979. (Available as J. Aircraft, May 1980, pp 332-38)
12. Su Wenhan, Liu Mouji, and Qiu Chenghao, "An Experimental Investigation of Spanwise Blowing," (in Chinese) BIAA, China, BH-B 850 1982.
13. Zhou Bocheng, Liu Mouji, Xiong Shanwen, and Li Zhifang," Vortex Flow Studies of a Strake — Wing in Water Tunnel", (in Chinese) BIAA, China, BH-B 851 1982.

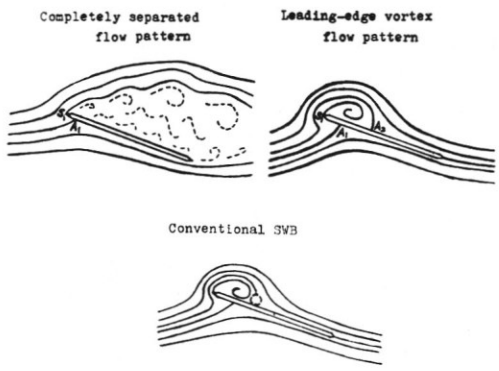

Fig.1 Two types of separated flow pattern and conventional SWB.

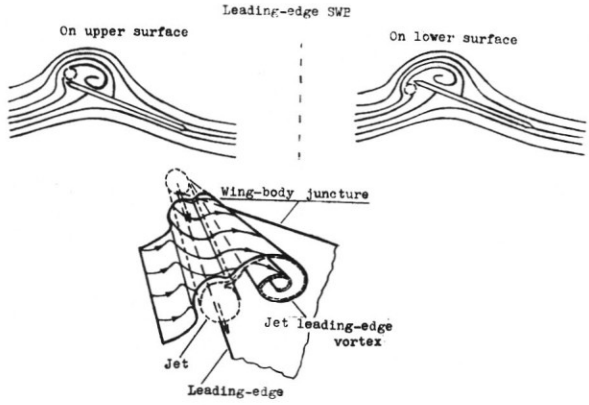

Fig.2 The leading-edge SWB.

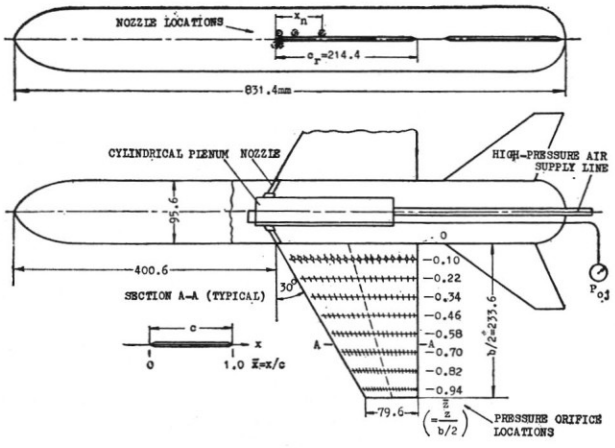

Fig.3 Wind tunnel model and air supply system.

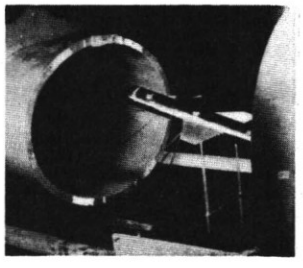

Fig.4 Photograph of model mounted in test section.

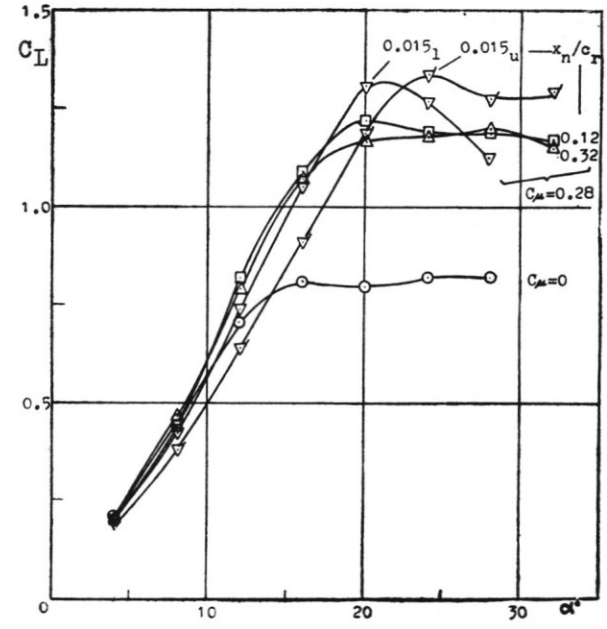

Fig.5 Effects of two types of spanwise blowing on wing lift characteristics.

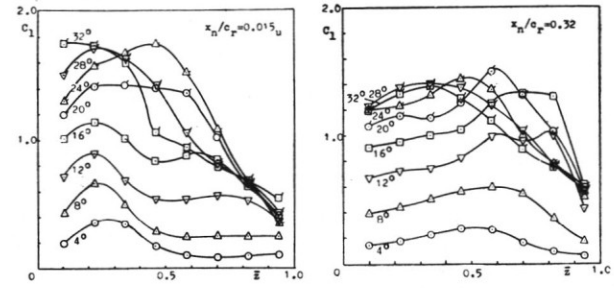

Fig.6 Variation of section lift coefficient along the span.

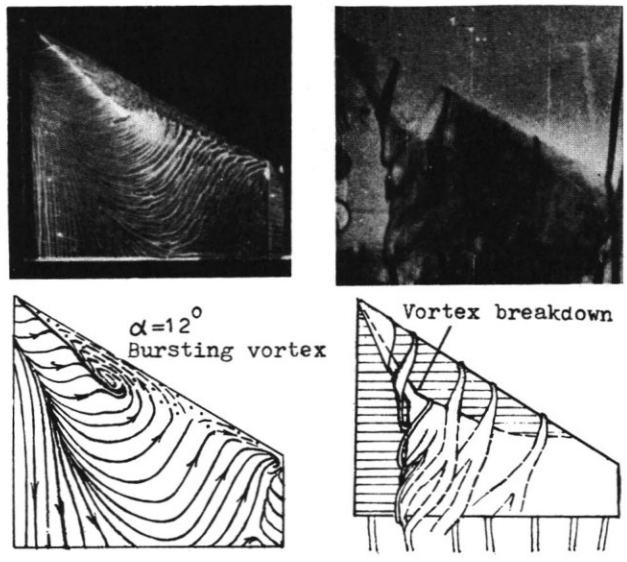

(a) bursting vortex

Fig.7 Typical flow patterns on upper surface of the wing without blowing.

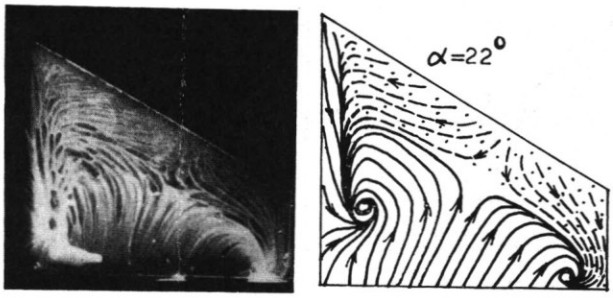

(b) spiral flow

Fig.7 Continued.

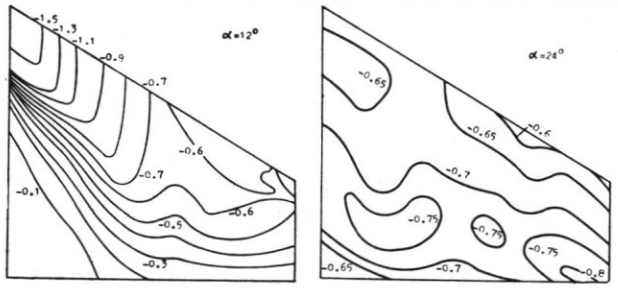

Fig.8 Typical upper surface pressure distributions of the wing without blowing.

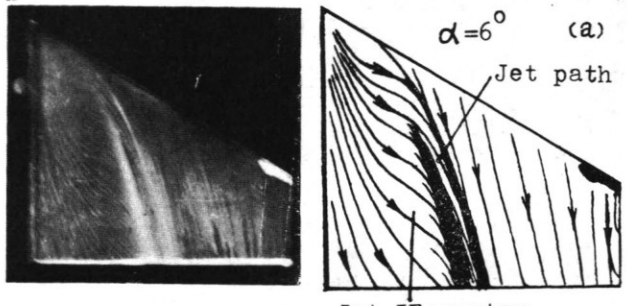

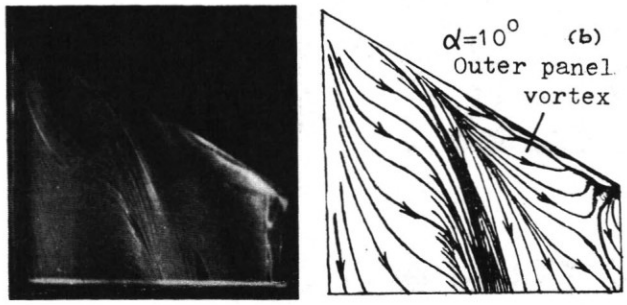

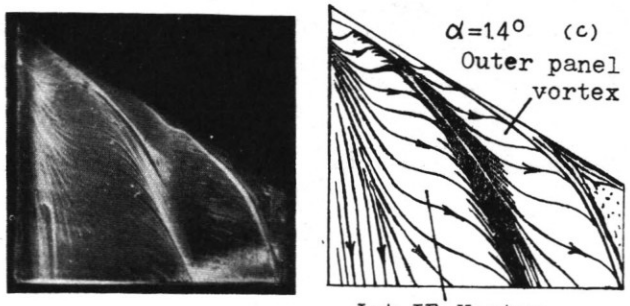

Fig.9 Flow patterns on upper surface of the wing with LE SWB for $x_n/c_r=0.015_u$.

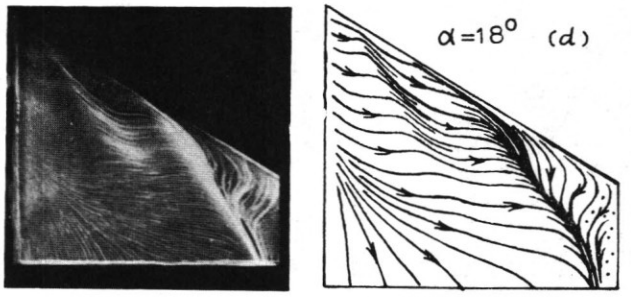

Jet LE/Outer panel vortex coalescence

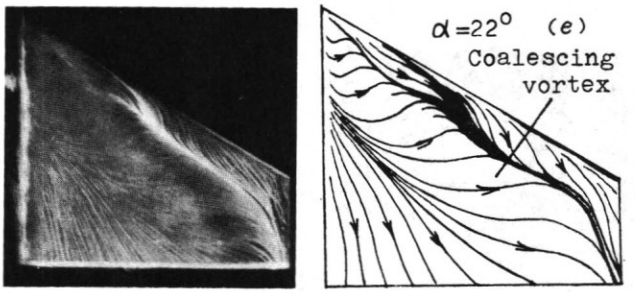

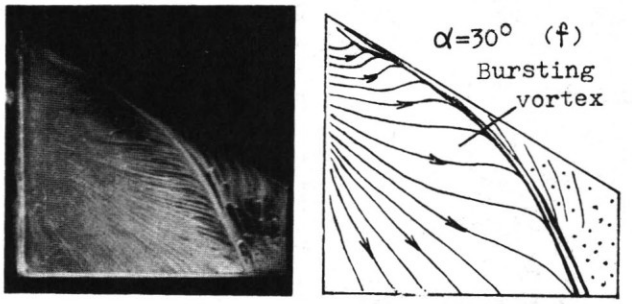

Fig.9 Continued.

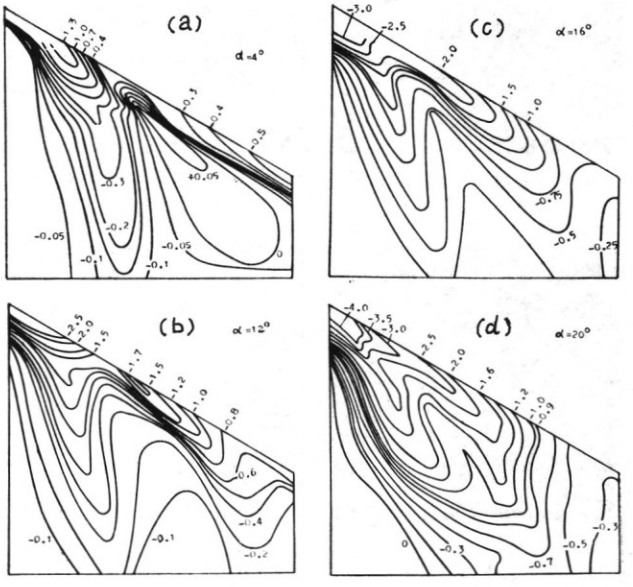

Fig.10 Upper surface pressure distributions of the wing with LE SWB for $x_n/c_r=0.015_u$.

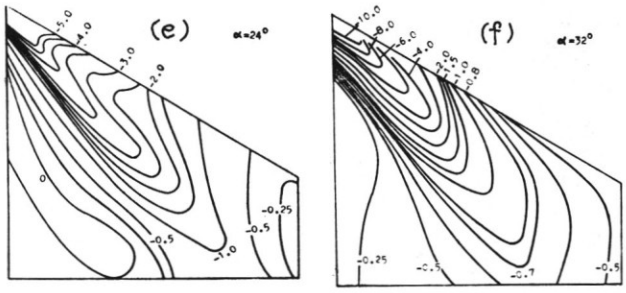

Fig.10 Continued.

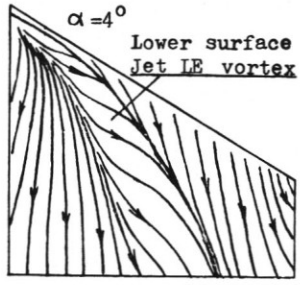

$\alpha=4^{\circ}$
Flow pattern and isobar pattern on lower surface.

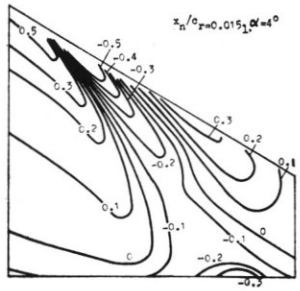

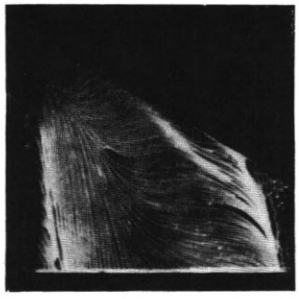

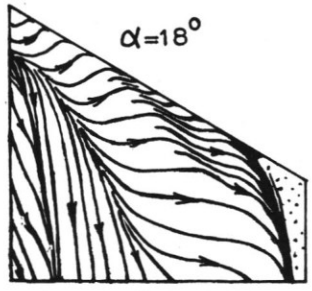

Jet LE/Outer panel vortex Coalescence

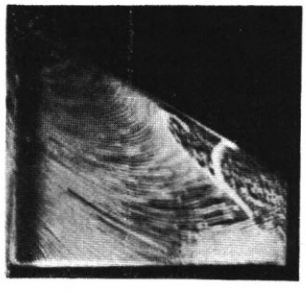

Flow patterns on upper surface($\alpha=18^{\circ}$ $\alpha=26^{\circ}$)

Fig.11a Flow patterns and related pressure distributions of the wing with LE SWB for $x_n/c_r=0.015_1$.

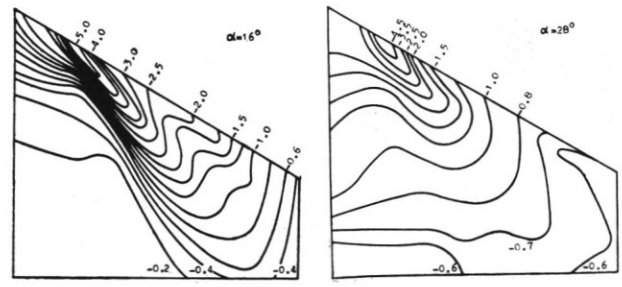

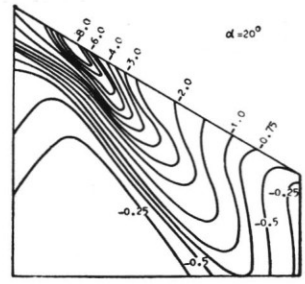

Isobar patterns on the upper surface.

Fig.11a Continued.

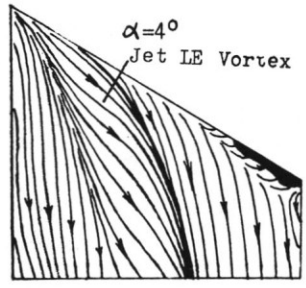

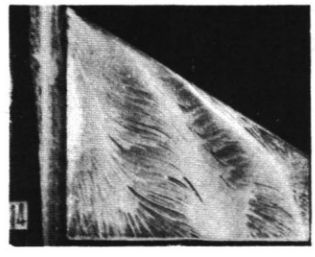

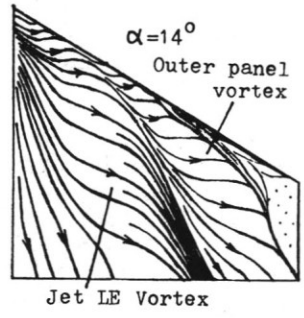

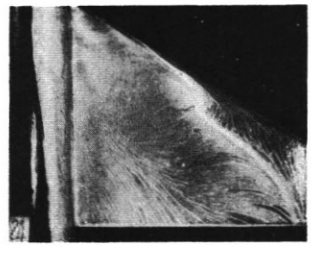

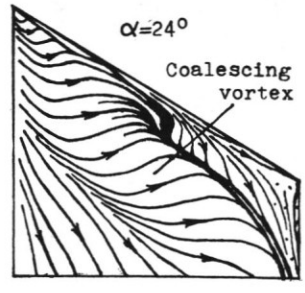

Fig.11b Flow patterns on upper surface of the wing with LE SWB for $x_n/c_r=0_1$

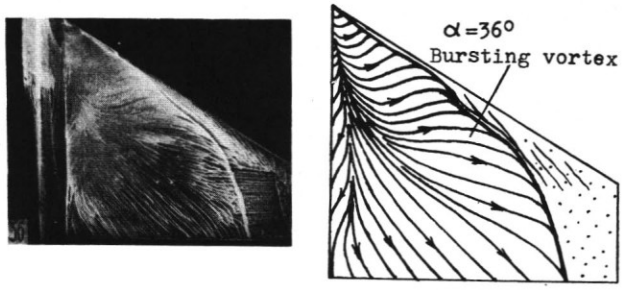

Fig.11b Continued.

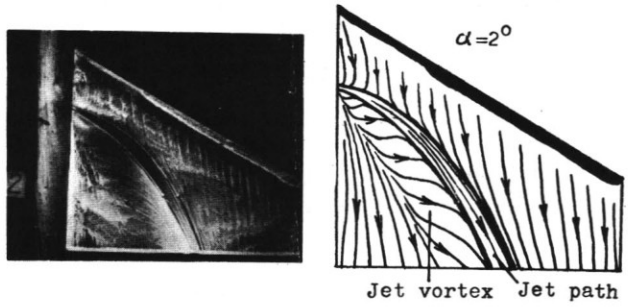

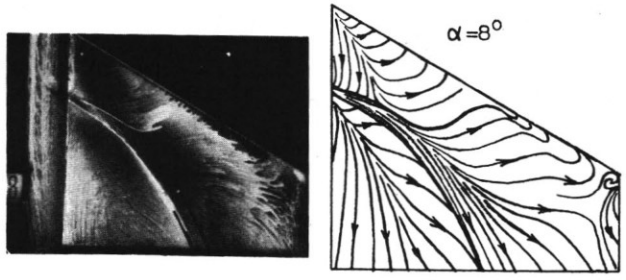

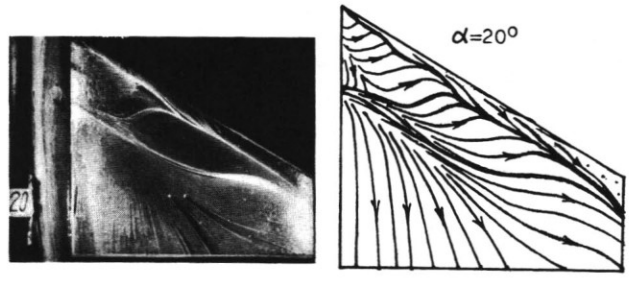

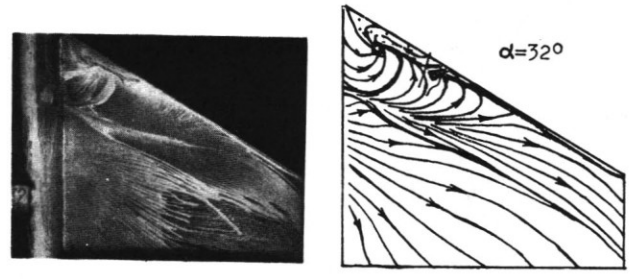

(a) surface flow patterns.

Fig.12 Typical flow patterns and pressure distributions of the wing upper surface for x_n/c_r=0.32.

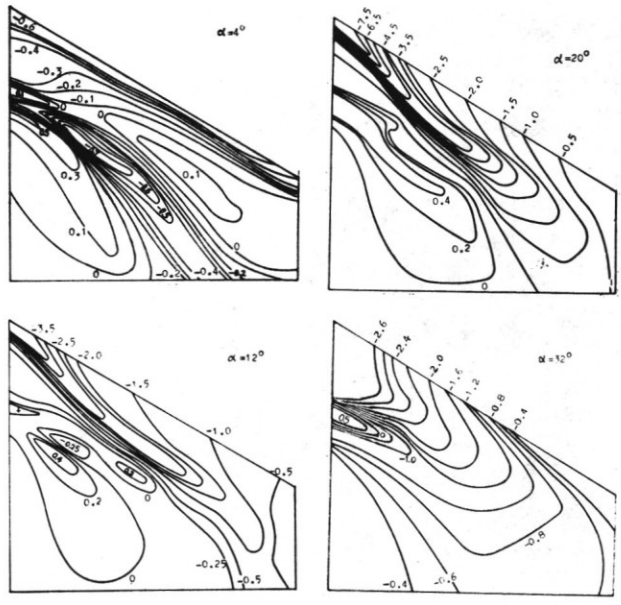

(b) Isobar patterns.

Fig.12 Continued.

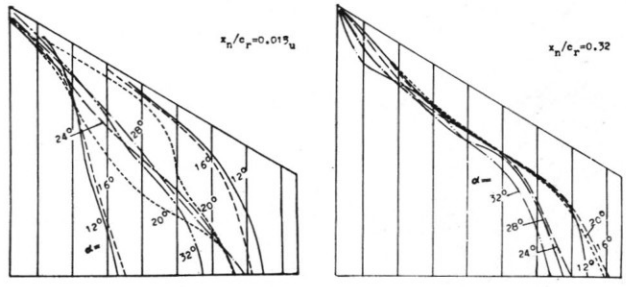

Fig.13 The positions of the suction ridge.

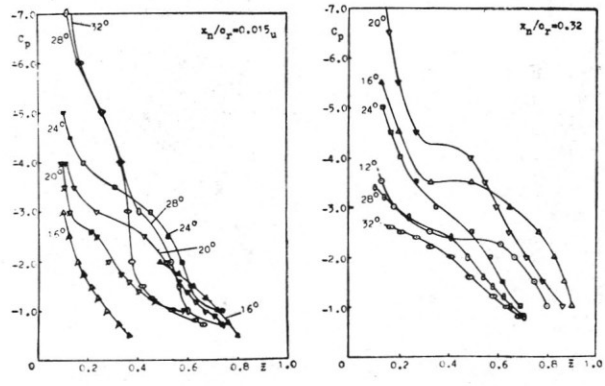

Fig.14 Surface pressure distribution along the suction ridge.

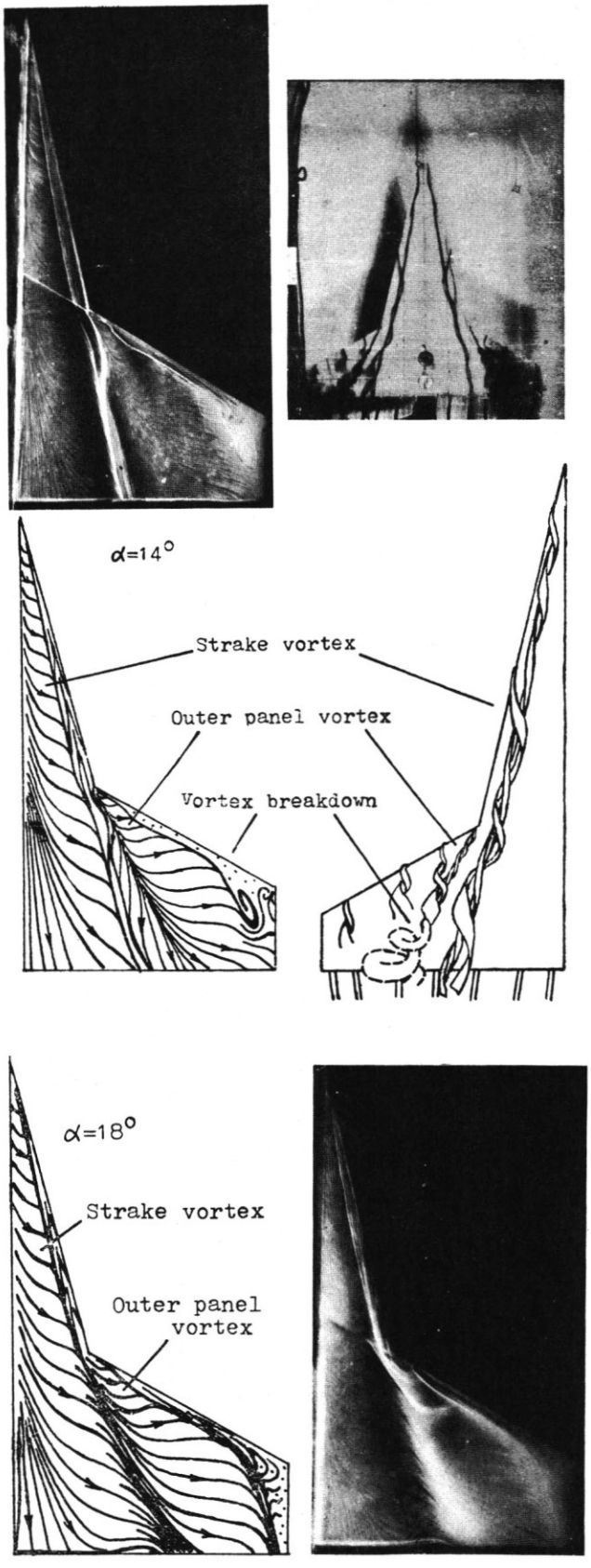

Fig.15 Typical flow patterns of the strake-wing.